



## Microwave Assisted Formation of Magnetic Core-Shell Carbon Nanostructure

Hongbo Gu,<sup>a,b</sup> Daowei Ding,<sup>a</sup> Pallavkar Sameer,<sup>a</sup> Jiang Guo,<sup>a</sup> Narendranath Yerra,<sup>a,c</sup> Yudong Huang,<sup>b</sup> Zhiping Luo,<sup>d</sup> Thomas C. Ho,<sup>a</sup> Neel Haldolaarachchige,<sup>e</sup> David P. Young,<sup>e</sup> Airat Khasanov,<sup>f</sup> Zhanhu Guo,<sup>a,\*</sup> and Suying Wei<sup>a,c,z</sup>

<sup>a</sup>Integrated Composites Lab (ICL), Dan F. Smith Department of Chemical Engineering, Lamar University, Beaumont, Texas 77710, USA

<sup>b</sup>School of Chemical Engineering and Technology, Harbin Institute of Technology, Harbin, 150001 Heilongjiang, China

<sup>c</sup>Department of Chemistry and Biochemistry, Lamar University, Beaumont, Texas 77710, USA

<sup>d</sup>Department of Chemistry and Physics and Southeastern North Carolina Regional Microanalytical and Imaging Consortium, Fayetteville State University, Fayetteville, North Carolina 28301, USA

<sup>e</sup>Department of Physics and Astronomy, Louisiana State University, Baton Rouge, Louisiana 70803, USA

<sup>f</sup>University of North Carolina at Asheville, Asheville, North Carolina 28804, USA

This letter describes a facile high temperature microwave assisted process to form the magnetic core-shell carbon nanostructure from polyaniline (PANI)-magnetite (Fe<sub>3</sub>O<sub>4</sub>) nanocomposites. The amorphous combined with graphitized carbon shell is observed by the transmission electron microscopy (TEM). The crystalline metallic iron, cementite, Fe<sub>3</sub>O<sub>4</sub> and iron oxide (Fe<sub>2</sub>O<sub>3</sub>) are observed in the magnetic core in the Mössbauer spectrum measurements. The increased magnetic properties are observed in the formed core-shell carbon nanostructure after microwave annealing. The formed solid carbon nanostructure can protect the material from the acid dissolution and magnetic core favors the recycling of material.

© 2013 The Electrochemical Society. [DOI: 10.1149/2.001312ssl] All rights reserved.

Manuscript submitted August 29, 2013; revised manuscript received September 12, 2013. Published September 19, 2013.

Recently, core-shell structure materials, especially for the magnetic core and protective shell materials, have gained more interests because the introduction of inert shell can provide a stabilized magnetic properties and oxidative resistance and protect the materials from the dissolution under acidic conditions.<sup>1-4</sup> They have the broadened potential applications such as catalysis,<sup>5,6</sup> giant magnetoresistance (GMR) sensing,<sup>7,8</sup> microwave absorption<sup>9,10</sup> and biomedical area.<sup>11,12</sup> Carbon materials are often introduced as shell materials to protect the magnetic metallic nanoparticles from oxidation/dissolution<sup>4,13</sup> and the synthesized magnetic core-shell structure materials have potential applications in magnetic data storage, ferrofluids magnetic hyperthermia and magnetic resonance imaging.<sup>14-16</sup>

The carbon coated magnetic nanoparticles are often fabricated by the chemical vapor deposition (CVD) method and the shell is formed by the annealing.<sup>4</sup> The conventional annealing method often uses hot-plates or thermal ovens to achieve the heating process and has many problems such as energy loss and low efficiency of energy usage.<sup>17</sup> Microwave annealing is an efficient and energy saving approach to heat materials,<sup>18</sup> and has been already used to synthesize the core-shell structure materials, such as Pd@Pt core-shell nanostructures,<sup>19</sup> core-shell Au-Pd bimetallic nanoparticles,<sup>20</sup> core-shell selenium-carbon colloids and hollow carbon capsules<sup>21</sup> and core-shell iron-carbon nanoparticles.<sup>22,23</sup> etc. Recently, it has been reported that the doped conducting polymer can rapidly lose heteroatoms, dopant ions, etc., and then convert to the graphitic nanocarbons after microwave heating method.<sup>24,25</sup> Based on these findings, we use the conducting polymer polyaniline (PANI) as the heating sources to form the carbon nanostructures.

In this work, we report on the facile high temperature (750–800°C) microwave-assisted approach to convert magnetite (Fe<sub>3</sub>O<sub>4</sub>)/PANI polymer nanocomposites (PNCs) into the magnetic core-shell carbon nanostructure. The synthesized magnetic core-shell carbon nanostructure is characterized by transmission electron microscopy (TEM), X-ray diffraction (XRD), room temperature Mössbauer spectra, thermogravimetric analysis (TGA), and magnetic property.

### Experimental

**Materials.**— Aniline (C<sub>6</sub>H<sub>7</sub>N), ammonium persulfate (APS, (NH<sub>4</sub>)<sub>2</sub>S<sub>2</sub>O<sub>8</sub>), p-toluene sulfonic acid (PTSA, C<sub>7</sub>H<sub>8</sub>O<sub>3</sub>S) were pur-

chased from Sigma Aldrich. Fe<sub>3</sub>O<sub>4</sub> NPs with an average size of 12 nm were obtained from Nanjing Emperor Nano Material Co., Ltd. All the chemicals were used as-received without any further treatment.

**Synthesis process.**— The Fe<sub>3</sub>O<sub>4</sub>/PANI nanocomposites were fabricated by surface initiated polymerization (SIP) method. Briefly, in the SIP method, the Fe<sub>3</sub>O<sub>4</sub> NPs (1.44 g, Nanjing Emperor Nano Material Co., Ltd., China), PTSA and APS (30.0 mmol and 18.0 mmol, respectively, Sigma Aldrich) were added into 200.0 mL deionized water in an ice-water bath for one hour of mechanical stirring combined with sonication. Then the aniline aqueous solution (Sigma Aldrich, 36.0 mmol in 50.0 mL deionized water) was mixed with the above Fe<sub>3</sub>O<sub>4</sub> nanoparticle suspension and mechanical and sonicated continuously for an additional hour in an ice-water bath for further polymerization. The product was vacuum filtered and washed with deionized water until the pH was about 7 and was further washed with methanol to remove any possible oligomers. The final PNC powders were dried at 50°C overnight.

The detailed information about microwave experimental setup and microwave annealing method is provided in the supporting information, SI.

**Characterization.**— The particle nanostructure was characterized by a transmission electron microscopy (TEM, FEI Tecnai G2 F20) with field emission gun, operated at an accelerating voltage of 200 kV. The TEM samples were prepared by drying a drop of samples/ethanol suspension on carbon-coated copper TEM grids. X-ray diffraction (XRD) analysis was carried out with a Bruker AXS D8 Discover diffractometer with GADDS (General Area Detector Diffraction System) operating with a Cu-K $\alpha$  radiation source filtered with a graphite monochromator ( $\lambda = 1.5406 \text{ \AA}$ ). Data were collected in a range of 10 to 70°. The Mössbauer spectrometer was set to produce a high precision Doppler velocity modulation of the source  $\gamma$  radiation. The effects of the Doppler velocity modulation on the absorption of  $\gamma$  radiation were recorded synchronously in the 1024 channels of the multichannel analyzer. The result was 1024 numbers representing registered gamma quanta (representing a singular quantum) passing through the absorber under the condition of different Doppler velocity. A separate calibration procedure establishes the exact correspondence channel-velocity (Spectrometer calibration is performed by measuring a standard a-Fe absorber, which produces a well known six line spectrum. The whole velocity range is calibrated using these six velocity points). The shape of the absorption spectrum was fitted to a theoretical model line shape.

\*Electrochemical Society Active Member.

<sup>z</sup>E-mail: suyong.wei@lamar.edu; zhanhu.guo@lamar.edu

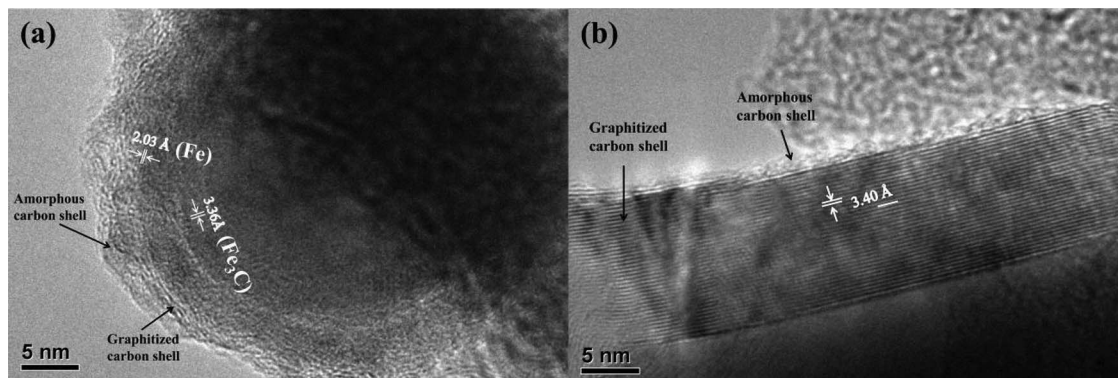


**Figure 1.** High resolution transmission electron microscopy (HRTEM) micrographs of microwave heat-assisted formed magnetic core-shell carbon nanostructure.

which was a superposition of singlets, doublets and sextets ( $^{57}\text{Fe}$  case) of a Lorentzian form. The result was investigated by chi 2 criterion and the theoretical line shape is tailored to fit experimental spectrum by the adjustment of spectral parameters like isomer shift, quadrupole splitting, hyperfine magnetic field and etc. Thermal stability of the synthesized nanocomposites was conducted in a thermogravimetric analysis (TGA, TA instruments, Q-500) with a heating rate of  $10^\circ\text{C min}^{-1}$  under an air flow rate of  $60\text{ mL min}^{-1}$  from  $25$  to  $800^\circ\text{C}$ . The room temperature Mössbauer spectra characterization is written in the SI. The magnetic properties were investigated in a 9-Tesla Physical Properties Measurement System (PPMS) by Quantum Design.

## Results and Discussion

Figure 1 shows the High resolution TEM microstructures of  $\text{Fe}_3\text{O}_4/\text{PANI}$  PNCs after high temperature microwave annealing. The core-shell structure is clearly shown in Figure 1a. The clear lattice fringe indicates the formation of highly crystalline nanoparticles. The calculated lattice distance of  $0.203\text{ nm}$  corresponds to  $(1\ 1\ 0)$  plane of iron and the lattice distance of  $0.336\text{ nm}$  is attributed to  $(0\ 2\ 0)$  plane of cementite ( $\text{Fe}_3\text{C}$ ).<sup>26</sup> The surrounding of magnetic core (cementite and iron) is uniformly coated by graphitized carbon layer (which is confirmed in Figure 1b, the lattice fringe space of  $0.34\text{ nm}$  corresponds to  $(0\ 0\ 2)$  plane of graphite carbon.) and a thin amorphous carbon layer. These results indicate that the high temperature microwave annealing favors the reduction of  $\text{Fe}_3\text{O}_4$  to metallic iron and the formation of cementite and the PANI has converted to carbon structure (graphitized carbon and amorphous carbon.) The XRD test is studied to further confirm the crystalline structure of the microwave heated core-shell carbon nanostructure and the result is shown in Figure S2. The observed corresponding XRD patterns of cementite and iron indicate the coexistence of the cementite and iron in this core-shell carbon nanostructure after microwave annealing. However, the XRD tests can't provide the detail information about the component of the magnetic core if the amount of the component is very less.

To precisely identify the specific components of the core structure, the room temperature Mössbauer spectra are measured and shown in Figure 2a. The fitting results show that there are five components in the core structure. The component 1 at isomer shift (IS) =  $0\text{ mm/s}$  corresponds to  $H_1 = 329\text{ kOe}$ , which represents to body centered cubic alpha-iron metallic magnetically ordered state<sup>27</sup> with a contribution of 28%. The component 2 with a contribution of 37% at IS =  $0.20$  and  $H_2 = 207\text{ kOe}$  is attributed to the cementite ( $\text{Fe}_3\text{C}$ ). The component 3 at IS =  $-0.07$  with a contribution of 23% corresponds to the alpha-iron, in which magnetic hyperfine structure has collapsed. The unusual change in electronic state IS =  $-0.07$  instead of IS =  $0$  indicates some decrease in d-electron density on iron. The component 4 with a contribution of 6% at IS =  $0.84$  and  $H_4 = 311\text{ kOe}$  indicates the presence of  $\text{Fe}_3\text{O}_4$ . The hyperfine field is much smaller

than the expected  $460\text{ kOe}$  due to the superparamagnetic relaxation in small particles. The component 5 with a contribution of 6% at IS =  $0.35$  and  $H_5 = 288\text{ kOe}$  corresponds to the  $\text{Fe}^{3+}$  in oxide environment ( $\text{Fe}_2\text{O}_3$ ) and the hyperfine field is much smaller than expected  $480\text{ kOe}$ , which is also due to the superparamagnetic relaxation in small particles. These results demonstrate that after high temperature microwave annealing, the formed magnetic core is composed of 4 components: alpha-iron, cementite,  $\text{Fe}_3\text{O}_4$  and  $\text{Fe}_2\text{O}_3$ . The observed iron, and cementite are consistent with the results of TEM, Figure 1a. Normally, cementite has reported mainly synthesized by laser pyrolysis and high temperature methods.<sup>28</sup> This conclusion is also confirmed in our work.

Figure 2b shows the TGA decomposition profiles of the  $\text{Fe}_3\text{O}_4/\text{PANI}$  PNCs and microwave assisted core-shell carbon nanostructures in the air condition. In the TGA curve, the  $\text{Fe}_3\text{O}_4/\text{PANI}$  PNCs have two-stage weight losses from  $250$  to  $600^\circ\text{C}$ , which are due to the elimination of the dopant anions and thermal degradation of PANI chains, respectively.<sup>29</sup> From the weight residue of the TGA curve, it's obtained that the  $\text{Fe}_3\text{O}_4$  nanoparticle loading in the  $\text{Fe}_3\text{O}_4/\text{PANI}$  PNCs is about  $34.05\text{ wt\%}$  for. However, after high temperature microwave annealing, the core-shell carbon nanostructures have two different decomposition profiles. The weight percentage of the core-shell carbon nanostructures increases to  $105.3\%$  as the temperature increases to  $407^\circ\text{C}$  which is due to the oxidation of iron in the air condition. After that, the weight loss of the core-shell carbon nanostructures starts and stops until temperature increases to  $680^\circ\text{C}$ . The weight residue of the final nanoparticles loading obtained from TGA is  $62.05\%$ . The high temperature microwave annealing carbonizes the PANI matrix and reduces the oxide shells. The mass loss and shrinkage of the PANI matrix effectively increases the particle loading for the final core-shell carbon nanostructures. The thermal stability of the formed core-shell carbon nanostructures ( $15\%$  weight loss is  $525^\circ\text{C}$ ) is obviously improved compared with the  $\text{Fe}_3\text{O}_4/\text{PANI}$  PNCs ( $15\%$  weight loss is  $339^\circ\text{C}$ ).

Figure 2c depicts the room temperature magnetization curves of the as-received  $\text{Fe}_3\text{O}_4$  nanoparticles,  $\text{Fe}_3\text{O}_4/\text{PANI}$  PNCs and microwave assisted core-shell carbon nanostructures. For the as-received  $\text{Fe}_3\text{O}_4$  nanoparticles and  $\text{Fe}_3\text{O}_4/\text{PANI}$  PNCs, there is no hysteresis loops observed in the curve, in which coercivity ( $H_c$ ) approaches zero Oe, exhibiting a superparamagnetic behavior.<sup>30</sup> Normally, the presence of an oxide shell around the metallic core is reported to increase the blocking temperature of nanoparticles through the exchange coupling interaction between the ferromagnetic metal core and the antiferromagnetic oxide shell.<sup>31</sup> Thus the reduction of  $\text{Fe}_3\text{O}_4$  to iron and the disappearance of exchange coupling in the microwave assisted core-shell carbon nanostructure should decrease the  $H_c$ . However, the  $H_c$  increases to  $78\text{ Oe}$  after high temperature microwave annealing. The increased  $H_c$  is attributed to the increased magnetic exchange coupling due to the presence of cementite.<sup>28</sup> The saturation magnetization ( $M_s$ ) of the as-received  $\text{Fe}_3\text{O}_4$  nanoparticles,  $\text{Fe}_3\text{O}_4/\text{PANI}$  PNCs and

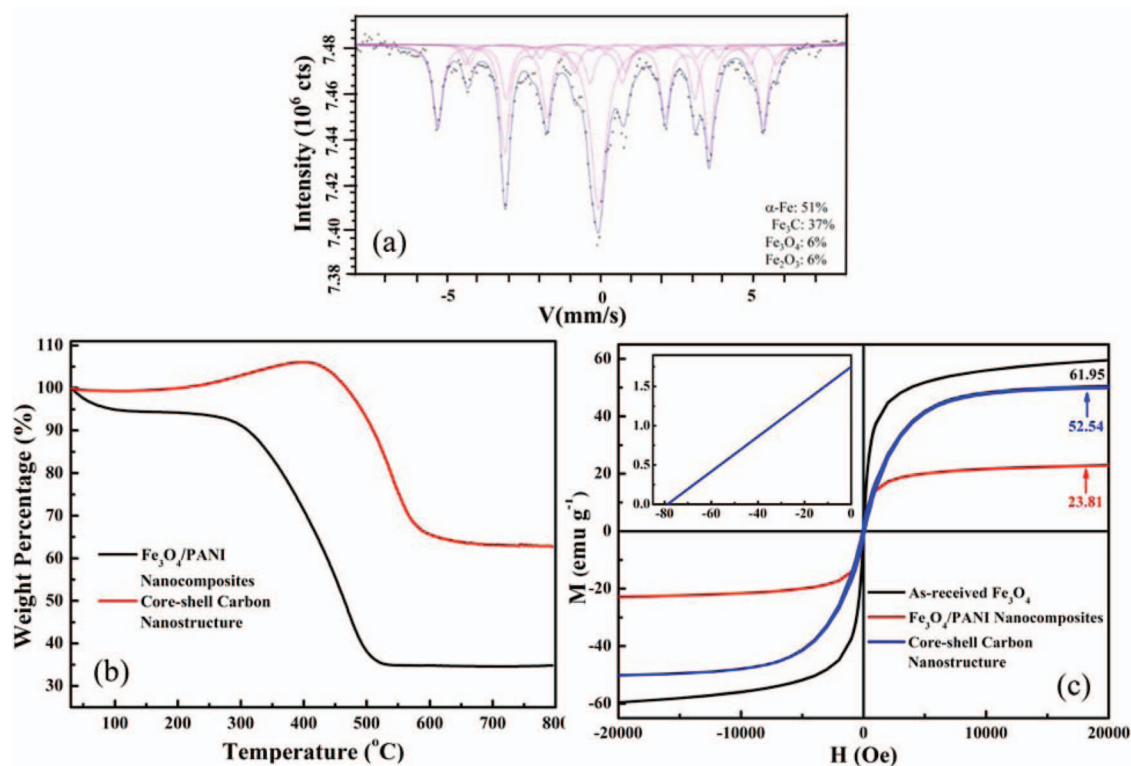


**Figure 2.** (a) Room temperature Mössbauer spectra of microwave heat assisted formed magnetic core-shell carbon nanostructure; (b) TGA curves of PANI/Fe<sub>3</sub>O<sub>4</sub> nanocomposites and microwave heat-assisted formed magnetic core-shell carbon nanostructure; (c) Magnetic properties of as-received Fe<sub>3</sub>O<sub>4</sub> nanoparticles, PANI/Fe<sub>3</sub>O<sub>4</sub> nanocomposites and microwave heat assisted formed magnetic core-shell carbon nanostructure.

microwave assisted core-shell carbon nanostructures is not reached even at high magnetic field and determined by the extrapolated saturation magnetization obtained from the intercept of  $M \sim H^{-1}$  at high field.<sup>32,33</sup> The calculated  $M_s$  of the as-received Fe<sub>3</sub>O<sub>4</sub> NPs is 61.95 emu g<sup>-1</sup>, which is lower than the bulk Fe<sub>3</sub>O<sub>4</sub> (92~100 emu g<sup>-1</sup>).<sup>34</sup> The  $M_s$  value of the Fe<sub>3</sub>O<sub>4</sub>/PANI is observed to be saturated at a lower field and is about 23.81 emu g<sup>-1</sup>. However, the  $M_s$  value of the microwave assisted core-shell structure is 52.54 emu g<sup>-1</sup>. The increased  $M_s$  value is attributed to the formed metallic iron and cementite, in which the pure bulk value is 222 emu g<sup>-1</sup> and 130 emu g<sup>-1</sup>, respectively.<sup>35,36</sup>

The acid stability of this microwave assisted core-shell carbon nanostructure was tested using 1 M HCl solution compared with samples synthesized by conventional annealing with the same condition. The results are shown in Figure S3. The microwave fabricated core-shell carbon nanostructure shows the solid structure and can protect the magnetic core from the acid dissolution. Meanwhile, it can be easily recycled by the permanent magnet, Figure S3-a. However, the conventional annealing fabricated sample has dissolved in the acid solution and produced many bubbles, which confirms the samples synthesized by conventional annealing is porous structure, Figure S3(b).

### Conclusions

In conclusion, we have fabricated core-shell carbon nanostructure from Fe<sub>3</sub>O<sub>4</sub>/PANI PNCs using the facile high temperature microwave assisted method. The microwave heat has carbonized the PANI matrix to graphitized carbon and amorphous carbon structure and formed the metallic iron, cementite, Fe<sub>2</sub>O<sub>3</sub> and Fe<sub>3</sub>O<sub>4</sub> magnetic core. The formed solid carbon nanostructure protects magnetic core from acid dissolution and magnetic core favors the easy recycle of this core-shell carbon nanostructure material. This core-shell carbon nanostructure has the potential applications in the environmental remediation application, especially in water treatment, e.g. the removal of heavy metals from polluted water.<sup>2,4</sup>

### Acknowledgments

This project is financially supported by the National Science Foundation through –Chemical and Biological Separations (CBET: 11–37441) and –Nanoscale Interdisciplinary Research Team, and Materials Processing and Manufacturing (CMMI 10–30755). D. P. Young acknowledges support from the National Science Foundation under grant No. DMR 10–05764. H. Gu acknowledges the support from China Scholarship Council (CSC) program.

### References

- H. Gu, S. Rapole, J. Sharma, Y. Huang, D. Cao, H. A. Colorado, Z. Luo, N. Haldolaarachchige, D. P. Young, S. Wei, and Z. Guo, *RSC Adv.*, **2**, 11007 (2012).
- D. Zhang, S. Wei, C. Kaila, X. Su, J. Wu, A. B. Karki, D. P. Young, and Z. Guo, *Nanoscale*, **2**, 917 (2010).
- J. Zhu, S. Wei, D. Rutman, N. Haldolaarachchige, D. P. Young, and Z. Guo, *Polymer*, **52**, 2947 (2011).
- S. Wei, Q. Wang, J. Zhu, L. Sun, H. Lin, and Z. Guo, *Nanoscale*, **3**, 4474 (2011).
- S. U. Son, Y. Jang, J. Park, H. B. Na, H. M. Park, H. J. Yun, J. Lee, and T. Hyeon, *J. Am. Chem. Soc.*, **126**, 5026 (2004).
- Y. Hou, Z. Xu, and S. Sun, *Angew. Chem. Int. Ed.*, **46**, 6329 (2007).
- Z. Guo, S. Park, H. T. Hahn, S. Wei, M. Moldovan, A. B. Karki, and D. P. Young, *Appl. Phys. Lett.*, **90**, 053111 (2007).
- S.-J. Cho, S. M. Kaulzarich, J. Olamit, K. Liu, F. Grandjean, L. Rebbouh, and G. J. Long, *J. Appl. Phys.*, **95**, 6804 (2004).
- J. Zhu, S. Wei, N. Haldolaarachchige, D. P. Young, and Z. Guo, *J. Phys. Chem. C*, **115**, 15304 (2011).
- X. Guo, Y. Deng, D. Gu, R. Che, and D. Zhao, *J. Mater. Chem.*, **19**, 6706 (2009).
- R. Hao, R. Xing, Z. Xu, Y. Hou, S. Gao, and S. Sun, *Adv. Mater.*, **22**, 2729 (2010).
- T.-J. Yoon, K. N. Yu, E. Kim, J. S. Kim, B. G. Kim, S.-H. Yun, B.-H. Sohn, M.-H. Cho, J.-K. Lee, and S. B. Park, *Small*, **2**, 209 (2006).
- M. Bystrzejewski, H. W. Hübers, A. Huczko, T. Gemming, B. Büchner, and M. H. Rümmeli, *Mater. Lett.*, **63**, 1767 (2009).
- M. E. McHenry, S. A. Majetich, J. O. Artman, M. DeGraef, and S. W. Staley, *Phys. Rev. B: Condens. Matter*, **49**, 11358 (1994).
- S. A. Majetich, J. O. Artman, M. E. McHenry, N. T. Nuhfer, and S. W. Staley, *Phys. Rev. B: Condens. Matter*, **48**, 16845 (1993).
- J.-P. Fortin, C. Wilhelm, J. Servais, C. Ménager, J.-C. Bacri, and F. Gazeau, *J. Am. Chem. Soc.*, **129**, 2628 (2007).

17. G. Li, V. Shrotriya, Y. Yao, and Y. Yang, *J. Appl. Phys.*, **98**, 043704 (2005).
18. C. J. Ko, Y. K. Lin, and F. C. Chen, *Adv. Mater.*, **19**, 3520 (2007).
19. H. Zhang, Y. Yin, Y. Hu, C. Li, P. Wu, S. Wei, and C. Cai, *J. Phys. Chem. C*, **114**, 11861 (2010).
20. R. Harpeness and A. Gedanken, *Langmuir*, **20**, 3431 (2004).
21. J. C. Yu, X. Hu, Q. Li, Z. Zheng, and Y. Xu, *Chem. Eur. J.*, **12**, 548 (2006).
22. Y.-C. Liang, K. C. Hwang, and S.-C. Lo, *Small*, **4**, 405 (2008).
23. Y.-L. Hsin, C.-F. Lin, Y.-C. Liang, K. C. Hwang, J.-C. Horng, J.-a. A. Ho, C.-C. Lin, and J. R. Hwu, *Adv. Funct. Mater.*, **18**, 2048 (2008).
24. X. Zhang and S. K. Manohar, *Chem. Commun.*, 2477 (2006).
25. Z. Liu, J. Wang, V. Kushvaha, S. Poyraz, H. Tippur, S. Park, M. Kim, Y. Liu, J. Bar, H. Chen, and X. Zhang, *Chem. Commun.*, **47**, 9912 (2011).
26. P. A. Carvalho, I. Fonseca, M. T. Marques, J. B. Correia, A. Almeida, and R. Vilar, *Acta Mater.*, **53**, 967 (2005).
27. J. Zhu, S. Wei, Y. Li, L. Sun, N. Haldolaarachchige, D. P. Young, C. Southworth, A. Khasanov, Z. Luo, and Z. Guo, *Macromolecules*, **44**, 4382 (2011).
28. M. D. Shultz, S. Calvin, F. Gonzalez-Jimenez, V. Mujica, B. C. Alleluia, and E. E. Carpenter, *Chem. Mater.*, **21**, 5594 (2009).
29. H. Gu, S. Tadakamalla, Y. Huang, H. A. Colorado, Z. Luo, N. Haldolaarachchige, D. P. Young, S. Wei, and Z. Guo, *ACS Appl. Mater. Interfaces*, **4**, 5613 (2012).
30. H. Gu, Y. Huang, X. Zhang, Q. Wang, J. Zhu, L. Shao, N. Haldolaarachchige, D. P. Young, S. Wei, and Z. Guo, *Polymer*, **53**, 801 (2012).
31. V. Skumryev, S. Stoyanov, Y. Zhang, G. Hadjipanayis, D. Givord, and J. Nogues, *Nature*, **423**, 850 (2003).
32. Z. Guo, L. L. Henry, V. Palshin, and E. J. Podlaha, *J. Mater. Chem.*, **16**, 1772 (2006).
33. D. Zhang, A. B. Karki, D. Rutman, D. P. Young, A. Wang, D. Cocke, T. H. Ho, and Z. Guo, *Polymer*, **50**, 4189 (2009).
34. P. Hu, S. Zhang, H. Wang, D. Pan, J. Tian, Z. Tang, and A. A. Volinsky, *J. Alloys Compd.*, **509**, 2316 (2011).
35. K. S. Suslick, M. Fang, and T. Hyeon, *J. Am. Chem. Soc.*, **118**, 11960 (1996).
36. B. David, O. Schneeweiss, M. Mashlan, E. Šantavá, and I. Morjan, *J. Magn. Magn. Mater.*, **316**, 422 (2007).